INSTITUT DE FRANCE
Académie des sciences

Comptes Rendus
Physique

Lei Ren, Cédric Robert, Bernhard Urbaszek, Xavier Marie, Marina Semina and Mikhail M. Glazov

Tuning absorption and emission in monolayer semiconductors: a brief survey

Volume 22, Special Issue S4 (2021), p. 43-52

Published online: 11 June 2021
Issue date: 8 March 2022

https://doi.org/10.5802/crphys.59

Part of Special Issue: Recent advances in 2D material physics
Guest editors: Xavier Marie (INSA Toulouse, Université Toulouse III Paul Sabatier, CNRS, France) and Johann Coraux (Institut Néel, Université Grenoble Alpes, CNRS, France)

Les Comptes Rendus. Physique *sont membres du Centre Mersenne pour l'édition scientifique ouverte*
www.centre-mersenne.org
e-ISSN : 1878-1535

Comptes Rendus
Physique
2021, 22, nº S4, p. 43-52
https://doi.org/10.5802/crphys.59

Recent advances in 2D material physics / *Physique des matériaux bidimensionnels*

Tuning absorption and emission in monolayer semiconductors: a brief survey

Lei Ren [a], Cédric Robert*, [a], Bernhard Urbaszek [a], Xavier Marie [a], Marina Semina [b] and Mikhail M. Glazov [b]

[a] Université de Toulouse, INSA-CNRS-UPS, LPCNO, Toulouse 31077, France

[b] Ioffe Institute, 26 Polytechnicheskaya, 194021 St. Petersburg, Russia

E-mails: ren@insa-toulouse.fr (L. Ren), cedric.robert@insa-toulouse.fr (C. Robert), urbaszek@insa-toulouse.fr (B. Urbaszek), marie@insa-toulouse.fr (X. Marie), msemina@gmail.com (M. Semina), glazov@coherent.ioffe.ru (M. M. Glazov)

Abstract. We review the physical mechanisms that allow tuning of absorption and emission characteristics in monolayer semiconductors. We use the model system of transition metal dichalcogenide mono-layers such as $MoSe_2$ or WSe_2 due to their very efficient light-matter interaction and availability of high quality samples. For monolayers encapsulated in hexagonal boron nitride both homogeneous and inhomogenous contributions to the exciton optical transition linewidth can be tuned opening up pathways for tailoring the reflectivity and absorption in van der Waals heterostructures.

Keywords. Transition metal dichalcogenide, Purcell effect, 2D materials, Electrodynamics, Coherent optics.

Available online 11th June 2021

Transition metal dichalcogenides (TMDs) such as $MoSe_2$ and WSe_2 are semiconducting layered materials [1, 2]. As the layers are coupled to each other by weak van der Waals bonding, it is possible to isolate single atomic layers by mechanical exfoliation using simple adhesive tape and investigate their two-dimensional (2D) electronic properties [3]. The optical properties of monolayer (ML) transition metal dichalcogenides are governed by robust excitons, electron-hole pairs bound by the Coulomb interaction [4]. The very efficient light matter interaction in these 2D semiconductors yields high absorption at excitonic resonance [5–7] and strong coupling for exciton–polaritons up to room temperature [8, 9]. In this paper, we review the recent results demonstrating the control of the radiative properties of 2D excitons in TMDs by placing them above a dielectric or a metallic mirror. While similar effects have been observed for individual localized emitters, such as atoms, ions, molecules or semiconductor quantum dots, near a mirror, the combination of delocalized 2D excitons in TMDs and planar mirror yield spectacular results owing to the high ratio of the radiative to non-radiative decay rates.

Let us recall that the optical response of the exciton can be discussed in the harmonic oscillator model, see, e.g., [10, 11]. The excitonic oscillator in this simple model can be described by three parameters: its energy E_0, its spectral linewidth γ and its oscillator strength or radiative linewidth

* Corresponding author.

γ_{rad}. As a result, the amplitude reflection coefficient of the monolayer at the normal incidence of light takes the form [10, 12, 13][1]

$$r = \frac{\mathrm{i}\gamma_{\mathrm{rad}}/2}{E_0 - E - \mathrm{i}\gamma/2}, \tag{1}$$

with the transmission coefficient and the monolayer absorbance being, respectively

$$t = 1 + r, \quad \text{and} \quad \mathscr{A} = 1 - |r|^2 - |t|^2. \tag{2}$$

In practice, the shape of the exciton response is a convolution between inhomogeneous γ_{inh} and homogeneous γ_{h} contributions: for comparable contributions, the total linewidth can be approximated by $\gamma \approx \gamma_{\mathrm{h}} + \gamma_{\mathrm{inh}}$, while the shape of the resonance is a convolution of a Lorentzian profile of linewidth γ_{h} and a Gaussian profile of linewidth γ_{inh}. On one hand, the inhomogeneous broadening γ_{inh} results from any kind of local potential due to chemical or structural fluctuations (for instance arising from impurities, defects, strain or local variations of the dielectric environment [14]) that creates an ensemble of oscillators with slightly different energies [15]. On the other hand, the homogeneous linewidth γ_{h} can be expressed as:

$$\gamma_{\mathrm{h}} = \frac{2\hbar}{T_2} \tag{3}$$

where T_2 is the coherence time during which the exciton state keeps a fixed phase with respect to the crystal ground state. The rate γ_{h} includes two contributions: the linewidth due to the population decay γ_1 and the linewidth due to pure dephasing processes γ^* [16].

$$\gamma_{\mathrm{h}} = \gamma_1 + \gamma^* = \frac{\hbar}{T_1} + \gamma^*. \tag{4}$$

Note that the factor 2 between Equations (3) and (4) stems from the fact that the coherence (defined by T_2) is proportional to the electric field while the population (defined by T_1) is proportional to the intensity of the electric field [17]. The exciton population decay can itself be separated into two recombination channels: either the radiative one characterized by the radiative decay rate $\gamma_{\mathrm{rad}} = \hbar/\tau_{\mathrm{rad}}$ or the non-radiative one with $\gamma_{\mathrm{nrad}} = \hbar/\tau_{\mathrm{nrad}}$ corresponding to trapping by defects, relaxation to other exciton states, non-radiative Auger recombination, etc., where τ_{rad} and τ_{nrad} are the radiative and the non-radiative lifetimes of the exciton, respectively. Note that the radiative component also defines the oscillator strength of the transition.

The pure dephasing term γ^* corresponds to any mechanism that breaks the coherence between the exciton state and the crystal ground state. It generally includes exciton–exciton scattering, exciton–phonon scattering [18, 19], or exciton–electron (exciton–hole) scattering in a doped sample.

These key parameters related to the damping of the exciton resonance can be distinguished in non-linear optical measurements such as four-wave mixing and photon echo experiments [20–25]. Thus homogeneous linewidths ranging from 0.2 meV to 3 meV have been reported for TMD ML exciton resonances. Interestingly, such a large γ_{h} is mainly due to the high oscillator strength of the excitons resulting in ps or sub-ps radiative lifetime τ_{rad} [26–29]. In most of the experimental studies on TMD monolayers before 2017, this *homogeneous* linewidth was, however, far smaller than the *inhomogeneous* broadening with values measured up to tens of meV. The improvement of sample quality by encapsulation of MLs in hBN considerably narrowed the exciton transitions down to 1 meV [30–32]. Thus TMD MLs are now ideal systems to reach a regime where the homogeneous contribution becomes dominant or at least is comparable with the inhomogeneous part making them superior to the state-of-the-art quantum well structures and comparable to the nuclear Mössbauer resonances in the X-ray range and superconducting qubits in the

[1] Note that the defined linewidths correspond here to the full width at half maximum that can be measured in the optical spectra.

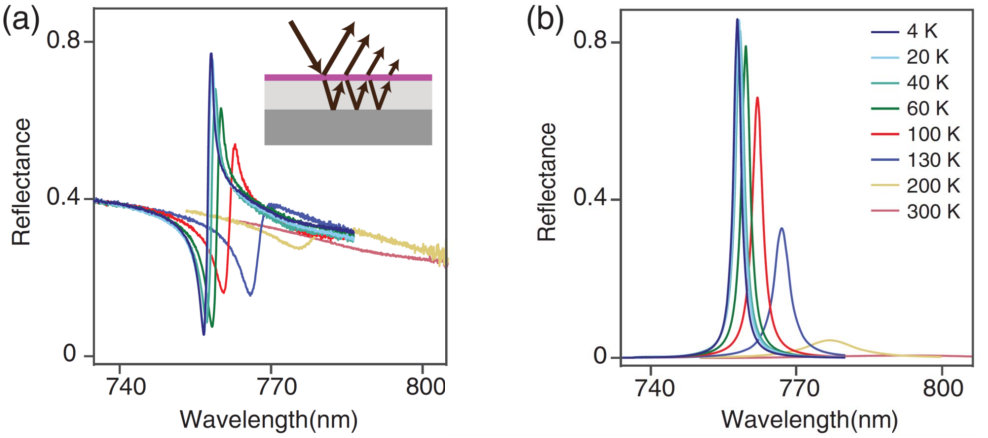

Figure 1. Temperature dependence of a $MoSe_2$ ML encapsulated into hBN showing near unity reflection at 4 K. Due to the surrounding dielectric layers (hBN, SiO_2) and the reflecting SiO_2/Si interface (see inset), the raw reflectance measurements (a) are affected by interference effects. (b) Reflectance of the ML corrected from the interference effects which corresponds to a fictional suspended ML. Adapted from [7] and reproduced with permission from [7]. Copyright 2018 American Physical Society.

microwave range [33–35]. This opens the way to fascinating studies of coherent optics and electrodynamical effects. Note that it is challenging to reach this regime in quasi-2D semiconductors such as GaAs quantum wells since the fluctuations of quantum well width introduce significant inhomogeneous broadening; the solution is then to investigate thick quantum wells where the fluctuations induce smaller inhomogenous broadening [36]. However in that case, the excitons loose their purely 2D properties [37].

One of the first manifestations of this coherent regime was given simultaneously by Back *et al.* and Scuri *et al.* in 2018 who demonstrated that a $MoSe_2$ ML encapsulated into hBN could reflect up to 85% when it is resonant with the bright exciton transition [6, 7]. The $MoSe_2$ ML thus acts as a nearly perfect atomically thin mirror. Figure 1b shows the measured reflectance corrected from the interference effects due to the surrounding dielectric layers as a function of the sample temperature (see inset of Figure 1a for a schematics of the sample). At a temperature of 4 K, the reflectance is larger than 80% as a direct consequence of the radiatively limited linewidth, i.e. γ_{rad} provides the main contribution to γ. Indeed, in absence of non-radiative decay and pure dephasing processes, the backward (forward) re-emitted light constructively (destructively) interfere with the resonant incident light so that reflectivity (transmission) reaches 100% (0%): It follows from (1) that in the optimal case of $\gamma = \gamma_{\text{rad}}$ the reflectivity at the resonance $E = E_0$ is $r = -1$ and, thus, $t = 0$. Such atomically thin mirrors represent the ultimate miniaturization limit of a reflective surface.

More recently, several studies have demonstrated the tuning of the radiative linewidth through the Purcell effect [13, 38–40]. The Purcell effect describes the modification of the spontaneous emission rate (i.e. of the radiative lifetime or linewidth) of a transition by the control of the density of electromagnetic modes in the environment. When a dipole is weakly coupled to a cavity mode, its emission rate is enhanced (reduced) if the transition is resonant (non-resonant) with the cavity modes [41–43].

One of the most direct demonstrations of the Purcell effect in TMD MLs was given by Fang *et al.* [13]. In this work, the authors considered a simple cavity-like structure composed of a $MoSe_2$ ML encapsulated in hBN top and bottom layers and deposited on a SiO_2/Si substrate (Figure 2a).

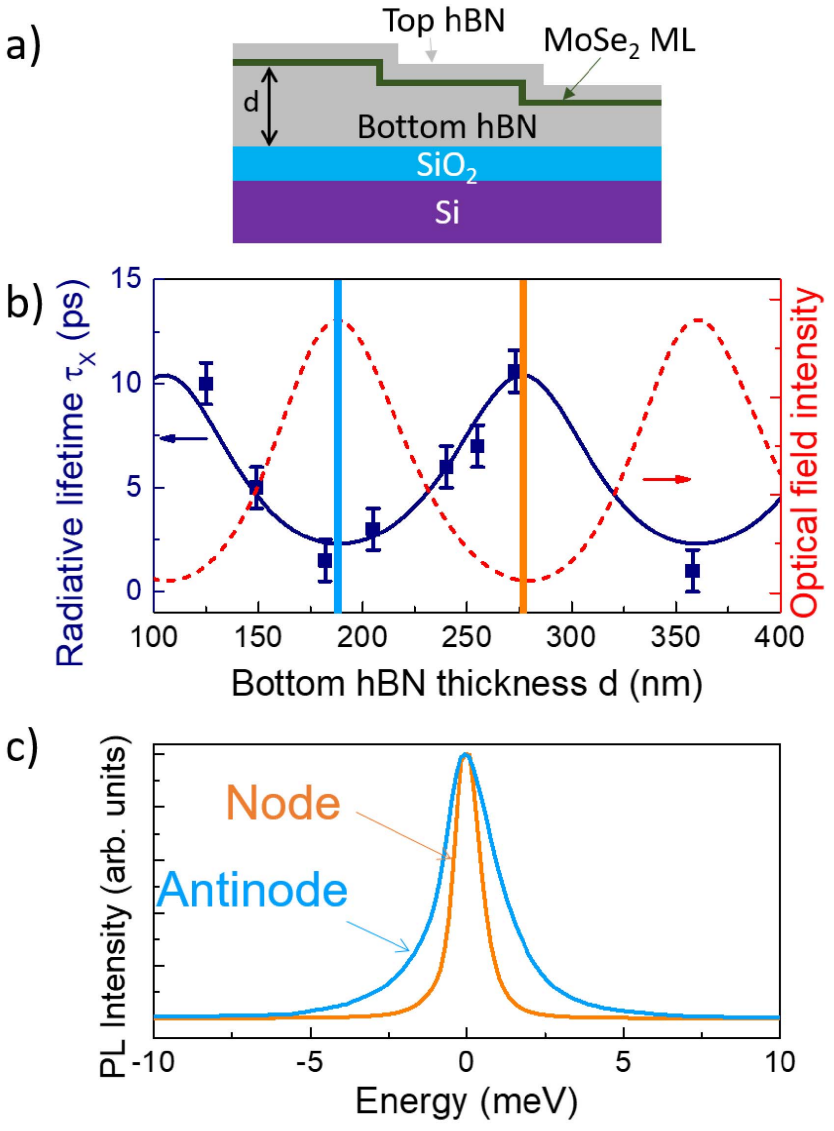

Figure 2. (a) Sketch of the van der Waals heterostructure used to observe the Purcell effect in [13]: a $MoSe_2$ ML is encapsulated between hBN layers with varying bottom hBN thickness. (b) Calculated (full line) and measured (symbols) neutral exciton radiative lifetime as a function of the hBN bottom layer thickness. The red dashed curve is the calculated intensity of the electromagnetic field in the ML. (c) Normalized cw PL intensity of the neutral exciton when the ML is located at the node and at the antinode of the optical field clearly showing different linewidths. Reproduced with permission from [13]. Copyright 2019 American Physical Society.

The SiO_2/Si interface plays the role of a partially reflective mirror. In this case the effective density of photon modes is simply tuned by varying the thickness of hBN layers (i.e. the distance between the ML and the SiO_2/Si interface). In other words, the electromagnetic field at the monolayer is enhanced by a factor $1 + r_b$ with r_b being the reflection coefficient of the composite hBN/SiO_2/Si substrate. As a result [13],

$$\gamma_{\mathrm{rad}} \rightarrow \gamma_{\mathrm{rad}}(1+\Re\{r_b\}), \tag{5}$$

with the Purcell factor $F_{\mathrm{p}} = 1+\Re\{r_b\}$ that can be larger or smaller than unity depending on the sign of $\Re\{r_b\}$. Using time-resolved photoluminescence spectroscopy, the authors measured a variation of the radiative lifetime of excitons by one order of magnitude (~1 ps to 10 ps), as shown in Figure 2b. The measured dependence is in very good agreement with the recombination rate calculated in the weak exciton–photon coupling regime: the red dashed curve displays the calculated intensity of the electromagnetic field at the position of the monolayer in the structure. When the ML is located at the antinode of the cavity mode, the radiative lifetime can be shortened by a factor up to two, as compared to the radiative lifetime of the exciton without the cavity (i.e. when the ML is embedded in infinitely thick hBN layers); this factor 2 is reached if we consider a perfectly reflective mirror instead of the SiO_2/Si interface, see Equation (5). In the opposite case, when the ML is located at the node of the optical field, significantly longer radiative lifetimes can be reached (this is the main effect observed in Figure 2b). Note that longer radiative lifetimes obtained in such conditions should facilitate the investigation of exciton–exciton interaction, Bose–Einstein condensates, optomechanical phenomena, etc... Nevertheless, as shown in Equation (4) an upper limit of the measurable exciton decay time T_1 is given by the non radiative lifetime τ_{nrad}. Among the non-radiative channels, relaxation to dark states are expected to play a major role. The choice of a TMD material with a ground bright state such as $MoSe_2$ is thus crucial.

Note that the Purcell effect can also be observed in the spectral domain. In Figure 2c, the modification of the total PL linewidth from 1.1 meV to 2.2 meV is clearly evidenced when the ML is placed respectively at the node and antinode of the optical field. This modification of the luminescence spectral width, due to the engineering of the exciton–photon weak coupling, was never observed in a semiconductor before to the best of our knowledge. Nevertheless the observed variation of amplitude of the linewidth is less than the measured variation of the lifetime because the lower limit of the linewidth is again given by the remaining inhomogeneous contributions (~1 meV). From an optoelectronic point of view, the tuning of the radiative lifetime through the Purcell effect can have a direct consequence on the luminescence efficiency of the TMD monolayers if the non-radiative lifetime due to defects lies in the tuning range of the radiative lifetime.

Another remarkable consequence of the electrodynamical effects in these 2D semiconductors is the possibility to tune the absorbance.[2] For an individual monolayer the absorbance follows from Equations (1) and (2) as [10]

$$\mathscr{A} = \frac{2\gamma_{\mathrm{rad}}(\gamma-\gamma_{\mathrm{rad}})}{4\delta^2+\gamma^2}. \tag{6}$$

Here $\delta = E - E_0$ is the detuning between the light frequency and the exciton resonance frequency, $\gamma' = \gamma - \gamma_{\mathrm{rad}}$ characterizes the non-radiative losses in the system. The maximal value of $\mathscr{A}$ reaches 1/2, i.e. 50% absorbance, and can be realized at the resonance conditions $E = E_0$ and $\gamma_{\mathrm{rad}} = \gamma/2$. In this case radiative, γ_{rad}, and other losses, γ', are balanced.

In van der Waals heterostructures the absorption can be made higher than that for an isolated ML, Equation (6), provided that destructive interferences can be arranged between the reflected/transmitted waves through the ML and the waves reflected from other interfaces in the heterostructure. To illustrate the effect let us consider the 2D TMD placed on the top of the reflective substrate with $|r_b| = 1$ and $t_b = 0$. The transmission coefficient of such a structure is 0,

[2] The dimensionless quantity $\mathscr{A}$ in (2) describes the fraction of incident energy absorbed by the 2D semiconductor, it is sometimes called the absorption coefficient. It should not be confused with the absorption coefficient α or inverse absorption length in Bouguer's law for the light propagation in bulk media.

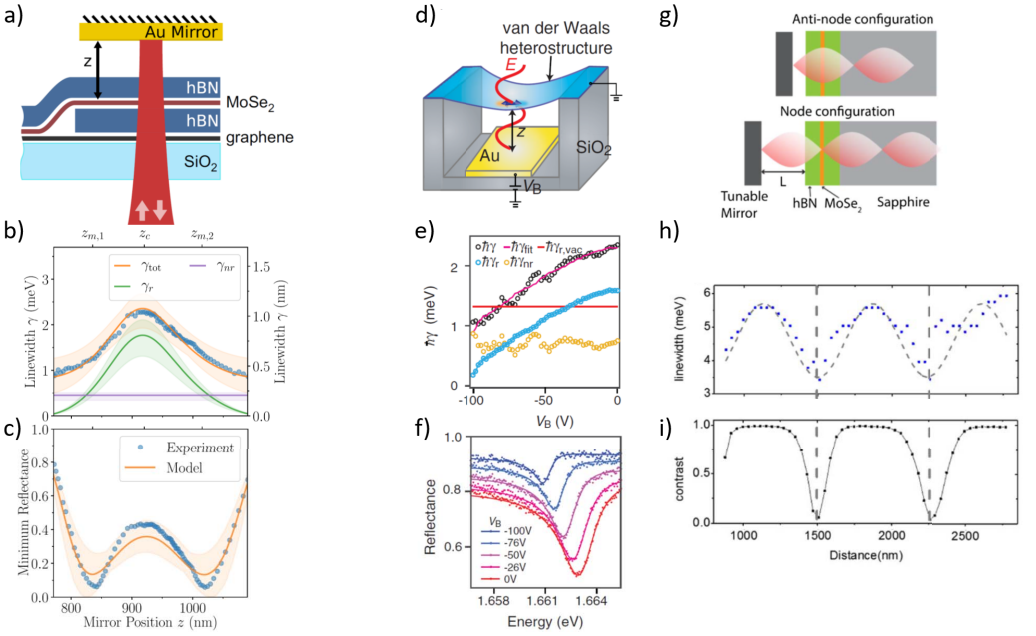

Figure 3. (a, d, g) Sketches of the samples used to demonstrate in-situ tuning of the radiative linewidth and of the absorption coefficient. (b, e, h) Corresponding variations of the radiative linewidth. (c, f, i) Corresponding vatiations of the reflectance. Adapted from [38, 39, 44]. In [39], the optical cavity mode is tuned by moving a Au mirror mounted on a mechanical actuator (a). (b, c) Measured linewidth and minimum reflectance as a function of the Au mirror position. The variation of the linewidth is due to the tuning of the radiative component γ_r while the non-radiative part γ_{nr} is constant. In [38], the ML is suspended above a Au mirror and its position is electrostatically controlled through the deformation of the membrane (d). (e, f) Measured linewidths and reflectance spectra as a function of the bias applied to the membrane. In [44], the device is very similar to (a) except that the tunable mirror is a DBR structure. (h, i) Measured linewidth and reflectance contrast as a function of the mirror distance. (a, b, c) Reproduced with permission from [39]. Copyright 2020 American Physical Society. (d, e, f) Reproduced with permission from [38]. Copyright 2020 American Physical Society. (g, h, i) Reprinted with permission from [44]. Copyright The Optical Society.

while the total reflectivity with accounts for the multiple reflections of light between the ML and the substrate reads [13]

$$r_{\text{tot}} = \frac{\mathrm{e}^{\mathrm{i}\phi}[2\delta + \mathrm{i}(\gamma' - \gamma_{\text{rad}})] - \mathrm{i}\gamma_{\text{rad}}}{2\delta + \mathrm{i}[\gamma' + \gamma_{\text{rad}}(1 + \mathrm{e}^{\mathrm{i}\phi})]}. \tag{7}$$

Here ϕ is the phase of the substrate reflection coefficient $r_b = \exp(\mathrm{i}\phi)$, which can be controlled, e.g., by the distance between the ML and the substrate. Remarkably, the absorbance $\mathscr{A} = 1 - |r_{\text{tot}}|^2$ can reach 100% under the condition that the reflectivity vanishes. The latter situation can be realized at

$$E = E_0 + \frac{\gamma_{\text{rad}} \sin\phi}{2}, \tag{8a}$$

$$\cos\phi = \frac{\gamma' - \gamma_{\text{rad}}}{\gamma_{\text{rad}}}. \tag{8b}$$

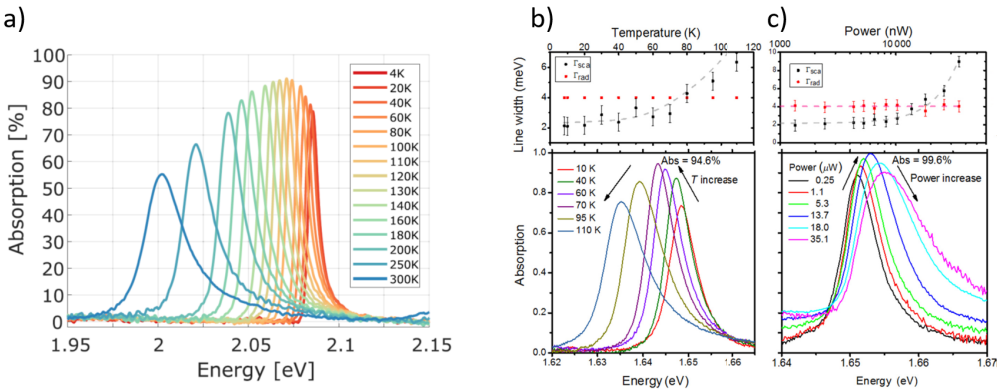

Figure 4. (a) Temperature dependence of the absorption of the neutral exciton in a WS_2 ML encapsulated in hBN and deposited on a gold mirror (adapted from [47]). The peak absorption is maximal at 110 K when both radiative and non-radiative linewidths are equal. (b, c) Temperature and laser power dependence of the absorption and linewidth of a $MoSe_2$ ML encapsulted in hBN and deposited on a DBR mirror (adapted from [40]). The peak absorption is maximal when both radiative Γ_{rad} and non-radiative Γ_{sca} linewidths are equal. (a) Reprinted with permission from [47]. Copyright 2020 American Chemical Society. (b, c) Reproduced with permission from [40]. Copyright 2020 American Physical Society.

The simultaneous fulfilment of the two conditions (8) implies also $|\gamma' - \gamma_{rad}| \leqslant \gamma_{rad}$ and requires, in general, both tuning of the linewidths of the exciton resonance and the distance between the monolayer and a mirror.

This regime of nearly perfect absorption has been demonstrated by several groups using different strategies to tune the radiative linewidth (Purcell effect) with respect to the non-radiative component [38–40]. In these three studies, the cavity modes were tuned in-situ either by using a mirror placed on a nanopositionner (Figures 3a and g) or by electrostatically moving the ML membrane on top of the mirror (Figure 3d). Using such a device, Rogers *et al.* [39] demonstrated a tuning of the radiative linewidth extracted from the modelling of the measured reflectivity spectra, from 1.8 meV to nearly zero (inhibition of the radiative rate) and of the absorption from zero to nearly unity (Figures 3b and c). Very similar results were obtained by Zhou *et al.* [38] with a tuning of the radiative linewidth between 1.6 meV and 0.19 meV (Figures 3e and f) while Horng *et al.* [40] measured a variation of the total linewidth from 2 to 5.5 meV and of the absorption from 4% to 99% (Figures 3h and i). Remarkably, a variation of the excitonic transition energy by 1 meV was observed that can be interpreted as a consequence of a cooperative Lamb shift [39, 40], evidenced previously with optical techniques in cold atoms or ions [45, 46]; it is well described by Equation (8a) in our model.

Absorption and emission properties can also be modified by tuning the non-radiative linewidth or the dephasing rate. To do so, one experimentally simple approach is to change the sample temperature. In Figure 4a, a maximum absorption as high as 92% is measured in a hBN-encapsulated WS_2 ML deposited on a gold mirror when the temperature is increased to 110 K. Note that the temperature at which maximum absorption is observed can be tuned using the Purcell effect (i.e. tuning γ_{rad}). Similar results were obtained by Horng *et al.* for a hBN-encapsulated $MoSe_2$ ML deposited on a Bragg mirror. By tuning the temperature or the laser power, the authors can change both non-radiative and dephasing rates (through exciton phonon or exciton–exciton scattering) and reach absorption as high as 99.6%, Figures 4b and c.

There are several interesting research prospects for the future. First, it has been predicted recently that engineering the dielectric environment also allows to control the exciton valley dynamics [48]. This would be a first direct engineering of the exciton exchange interactions for reducing the spin/valley depolarization mechanism. Second, there are other approaches in photonics to change locally the optical field experienced by the monolayer. For instance TMDs can be coupled to plasmonic or dielectric nanoresonators to achieve this effect [49–51]. The material challenge in that case is to maintain high sample quality, so that homogenous and inhomogenous contributions to the linewidth can be distinguished. Also, interpreting only time-resolved experiments is challenging due to the complex interplay of intrinsic radiative recombination mechanisms with fast non-radiative channels requiring an analysis based on the comparison between the temporal dynamics and spectral properties of the excitons.

Acknowledgements

This work was supported by Agence Nationale de la Recherche funding ANR 2D-vdW-Spin, ANR VallEx and ANR MagicValley and the French-Russian IRP PHYNICS, CNRS and RFBR joint Project No. 20-52-16303.

References

[1] J. Wilson, A. Yoffe, "The transition metal dichalcogenides discussion and interpretation of the observed optical, electrical and structural properties", *Adv. Phys.* **18** (1969), no. 73, p. 193-335.
[2] V. Kalikhman, Y. S. Umanski, "Transition-metal chalcogenides with layer structures and features of the filling of their Brillouin zones", *Sov. Phys. Uspekhi* **15** (1973), no. 6, p. 728-741.
[3] K. F. Mak, C. Lee, J. Hone, J. Shan, T. F. Heinz, "Atomically thin MoS_2: a new direct-gap semiconductor", *Phys. Rev. Lett.* **105** (2010), no. 13, article no. 136805.
[4] G. Wang, A. Chernikov, M. M. Glazov, T. F. Heinz, X. Marie, T. Amand, B. Urbaszek, "Colloquium: excitons in atomically thin transition metal dichalcogenides", *Rev. Mod. Phys.* **90** (2018), article no. 021001.
[5] Y. Li, A. Chernikov, X. Zhang, A. Rigosi, H. M. Hill, A. M. Van Der Zande, D. A. Chenet *et al.*, "Measurement of the optical dielectric function of monolayer transition-metal dichalcogenides: MoS_2, $MoSe_2$, WS_2, and WSe_2", *Phys. Rev. B* **90** (2014), no. 20, article no. 205422.
[6] P. Back, S. Zeytinoglu, A. Ijaz, M. Kroner, A. Imamoğlu, "Realization of an electrically tunable narrow-bandwidth atomically thin mirror using monolayer $MoSe_2$", *Phys. Rev. Lett.* **120** (2018), article no. 037401.
[7] G. Scuri, Y. Zhou, A. A. High, D. S. Wild, C. Shu, K. De Greve *et al.*, "Large excitonic reflectivity of monolayer $MoSe_2$ encapsulated in hexagonal boron nitride", *Phys. Rev. Lett.* **120** (2018), article no. 037402.
[8] X. Liu, T. Galfsky, Z. Sun, F. Xia, E.-C. Lin, Y.-H. Lee, S. Kéna-Cohen, V. M. Menon, "Strong light–matter coupling in two-dimensional atomic crystals", *Nat. Photonics* **9** (2015), no. 1, p. 30-34.
[9] S. Dufferwiel *et al.*, "Exciton–polaritons in van der Waals heterostructures embedded in tunable microcavities", *Nat. Commun.* **6** (2015), no. 1, p. 1-7.
[10] E. L. Ivchenko, *Optical Spectroscopy of Semiconductor Nanostructures*, Alpha Science, Harrow, UK, 2005.
[11] C. Schneider, M. M. Glazov, T. Korn, S. Höfling, B. Urbaszek, "Two-dimensional semiconductors in the regime of strong light-matter coupling", *Nat. Commun.* **9** (2018), no. 1, article no. 2695.
[12] M. M. Glazov, T. Amand, X. Marie, D. Lagarde, L. Bouet, B. Urbaszek, "Exciton fine structure and spin decoherence in monolayers of transition metal dichalcogenides", *Phys. Rev. B* **89** (2014), no. 20, article no. 201302.
[13] H. H. Fang, B. Han, C. Robert, M. A. Semina, D. Lagarde, E. Courtade, T. Taniguchi *et al.*, "Control of the exciton radiative lifetime in van der Waals Heterostructures", *Phys. Rev. Lett.* **123** (2019), article no. 067401.
[14] A. Raja *et al.*, "Dielectric disorder in two-dimensional materials", *Nat. Nanotechnol.* **14** (2019), no. 9, p. 832-837.
[15] L. C. Andreani, G. Panzarini, A. V. Kavokin, M. R. Vladimirova, "Effect of inhomogeneous broadening on optical properties of excitons in quantum wells", *Phys. Rev. B* **57** (1998), p. 4670-4680.
[16] L. Schultheis, A. Honold, J. Kuhl, K. Köhler, C. W. Tu, "Optical dephasing of homogeneously broadened two-dimensional exciton transitions in GaAs quantum wells", *Phys. Rev. B* **34** (1986), p. 9027-9030.
[17] R. T. Phillips (ed.), *Coherent Optical Interactions in Semiconductors*, Nato Science Series B, Springer, 1994, https://www.springer.com/gp/book/9780306447372 (accessed 22nd February 2021).
[18] D. Christiansen, M. Selig, G. Berghäuser, R. Schmidt, I. Niehues, R. Schneider, A. Arora *et al.*, "Phonon sidebands in monolayer transition metal dichalcogenides", *Phys. Rev. Lett.* **119** (2017), article no. 187402.

[19] S. Shree, M. Semina, C. Robert, B. Han, T. Amand, A. Balocchi *et al.*, "Observation of exciton-phonon coupling in $MoSe_2$ monolayers", *Phys. Rev. B* **98** (2018), article no. 035302.
[20] G. Moody *et al.*, "Intrinsic homogeneous linewidth and broadening mechanisms of excitons in monolayer transition metal dichalcogenides", *Nat. Commun.* **6** (2015), no. 1, p. 1-6.
[21] T. Jakubczyk, V. Delmonte, M. Koperski, K. Nogajewski, C. Faugeras, W. Langbein *et al.*, "Radiatively limited dephasing and exciton dynamics in $MoSe_2$ monolayers revealed with four-wave mixing microscopy", *Nano Lett.* **16** (2016), no. 9, p. 5333-5339.
[22] T. Jakubczyk, K. Nogajewski, M. R. Molas, M. Bartos, W. Langbein, M. Potemski, J. Kasprzak, "Impact of environment on dynamics of exciton complexes in a WS_2 monolayer", *2D Mater.* **5** (2018), no. 3, article no. 031007.
[23] T. Jakubczyk *et al.*, "Coherence and density dynamics of excitons in a single-layer MoS_2 reaching the homogeneous limit", *ACS Nano* **13** (2019), no. 3, p. 3500-3511.
[24] C. Boule, D. Vaclavkova, M. Bartos, K. Nogajewski, L. Zdražil, T. Taniguchi *et al.*, "Coherent dynamics and mapping of excitons in single-layer $MoSe_2$ and WSe_2 at the homogeneous limit", *Phys. Rev. Mater.* **4** (2020), no. 3, article no. 034001.
[25] E. W. Martin, J. Horng, H. G. Ruth, E. Paik, M.-H. Wentzel, H. Deng, S. T. Cundiff, "Encapsulation narrows and preserves the excitonic homogeneous linewidth of exfoliated monolayer $MoSe_2$", *Phys. Rev. Appl.* **14** (2020), no. 2, article no. 021002.
[26] D. Lagarde, L. Bouet, X. Marie, C. Zhu, B. Liu, T. Amand, P. Tan, B. Urbaszek, "Carrier and polarization dynamics in monolayer MoS_2", *Phys. Rev. Lett.* **112** (2014), no. 4, article no. 047401.
[27] C. Robert, D. Lagarde, F. Cadiz, G. Wang, B. Lassagne, T. Amand *et al.*, "Exciton radiative lifetime in transition metal dichalcogenide monolayers", *Phys. Rev. B* **93** (2016), article no. 205423.
[28] M. Palummo, M. Bernardi, J. C. Grossman, "Exciton radiative lifetimes in two-dimensional transition metal dichalcogenides", *Nano Lett.* **15** (2015), no. 5, p. 2794-2800.
[29] H. Wang, C. Zhang, W. Chan, C. Manolatou, S. Tiwari, F. Rana, "Radiative lifetimes of excitons and trions in monolayers of the metal dichalcogenide MoS_2", *Phys. Rev. B* **93** (2016), article no. 045407.
[30] F. Cadiz, E. Courtade, C. Robert, G. Wang, Y. Shen, H. Cai, T. Taniguchi, K. Watanabe *et al.*, "Excitonic linewidth approaching the homogeneous limit in MoS_2-based van der Waals Heterostructures", *Phys. Rev. X* **7** (2017), article no. 021026.
[31] O. A. Ajayi *et al.*, "Approaching the intrinsic photoluminescence linewidth in transition metal dichalcogenide monolayers", *2D Mater.* **4** (2017), no. 3, article no. 031011.
[32] J. Wierzbowski *et al.*, "Direct exciton emission from atomically thin transition metal dichalcogenide heterostructures near the lifetime limit", *Sci. Rep.* **7** (2017), no. 1, p. 1-6.
[33] E. L. Ivchenko, A. N. Poddubny, "Resonant diffraction of electromagnetic waves from solids (a review)", *Phys. Solid State* **55** (2013), no. 5, p. 905-923.
[34] O. Astafiev, A. M. Zagoskin, A. A. Abdumalikov, Y. A. Pashkin *et al.*, "Resonance fluorescence of a single artificial atom", *Science* **327** (2010), no. 5967, p. 840-843.
[35] I. S. Besedin, M. A. Gorlach, N. N. Abramov, I. Tsitsilin, I. N. Moskalenko, A. A. Dobronosova *et al.*, "Topological photon pairs in a superconducting quantum metamaterial", 2020, preprint, https://arxiv.org/abs/2006.12794.
[36] B. Jusserand, A. N. Poddubny, A. V. Poshakinskiy, A. Fainstein, A. Lemaitre, "Polariton resonances for ultrastrong coupling cavity optomechanics in GaAs/AlAs multiple quantum wells", *Phys. Rev. Lett.* **115** (2015), article no. 267402.
[37] H. Gibbs, G. Khitrova, S. W. Koch, "Exciton–polariton light–semiconductor coupling effects", *Nat. Photonics* **5** (2011), no. 5, p. 275-282.
[38] Y. Zhou, G. Scuri, J. Sung, R. J. Gelly, D. S. Wild, K. De Greve, A. Y. Joe *et al.*, "Controlling excitons in an atomically thin membrane with a mirror", *Phys. Rev. Lett.* **124** (2020), article no. 027401.
[39] C. Rogers, D. Gray, N. Bogdanowicz, T. Taniguchi, K. Watanabe, H. Mabuchi, "Coherent feedback control of two-dimensional excitons", *Phys. Rev. Res.* **2** (2020), article no. 012029.
[40] J. Horng, E. W. Martin, Y.-H. Chou, E. Courtade, T.-C. Chang, C.-Y. Hsu, M.-H. Wentzel *et al.*, "Perfect absorption by an atomically thin crystal", *Phys. Rev. Appl.* **14** (2020), article no. 024009.
[41] K. Drexhage, "Influence of a dielectric interface on fluorescence decay time", *J. Lumin.* **1** (1970), p. 693-701.
[42] D. Kleppner, "Inhibited spontaneous emission", *Phys. Rev. Lett.* **47** (1981), no. 4, p. 233-236.
[43] W. Jhe, A. Anderson, E. Hinds, D. Meschede, L. Moi, S. Haroche, "Suppression of spontaneous decay at optical frequencies: Test of vacuum-field anisotropy in confined space", *Phys. Rev. Lett.* **58** (1987), no. 7, p. 666-669.
[44] J. Horng, Y.-H. Chou, Y.-H. Chou, T.-C. Chang, C.-Y. Hsu, T.-C. Lu, H. Deng *et al.*, "Engineering radiative coupling of excitons in 2D semiconductors", *Optica* **6** (2019), no. 11 (EN), p. 1443-1448.
[45] J. Keaveney, A. Sargsyan, U. Krohn, I. G. Hughes, D. Sarkisyan, C. S. Adams, "Cooperative Lamb shift in an atomic vapor layer of nanometer thickness", *Phys. Rev. Lett.* **108** (2012), no. 17, article no. 173601.
[46] T. Peyrot, Y. Sortais, A. Browaeys, A. Sargsyan, D. Sarkisyan, J. Keaveney, I. Hughes, C. S. Adams, "Collective Lamb shift of a nanoscale atomic vapor layer within a sapphire cavity", *Phys. Rev. Lett.* **120** (2018), no. 24, article no. 243401.

[47] I. Epstein *et al.*, "Near-unity light absorption in a monolayer WS_2 van der Waals heterostructure cavity", *Nano Lett.* **20** (2020), no. 5, p. 3545-3552.

[48] A. I. Prazdnichnykh, M. M. Glazov, L. Ren, C. Robert, B. Urbaszek, X. Marie, "Control of the exciton valley dynamics in van der Waals heterostructures", *Phys. Rev. B* **103** (2021), article no. 085302.

[49] J. Kern *et al.*, "Nanoantenna-enhanced light–matter interaction in atomically thin WS_2", *ACS Photonics* **2** (2015), no. 9, p. 1260-1265.

[50] S. Bidault, M. Mivelle, N. Bonod, "Dielectric nanoantennas to manipulate solid-state light emission", *J. Appl. Phys.* **126** (2019), no. 9, article no. 094104.

[51] J.-M. Poumirol, I. Paradisanos, S. Shree, G. Agez, X. Marie, C. Robert, N. Mallet, P. R. Wiecha *et al.*, "Unveiling the optical emission channels of monolayer semiconductors coupled to silicon nanoantennas", *ACS Photonics* **7** (2020), no. 11, p. 3106-3115.